DOI: 10.1002/anie.201407475

Luminescence

Bimetallic Cyclometalated Iridium(III) Diastereomers with Non-Innocent Bridging Ligands for High-Efficiency Phosphorescent OLEDs**

Yonghao Zheng, Andrei S. Batsanov, Mark A. Fox, Hameed A. Al-Attar, Khalid Abdullah, Vygintas Jankus, Martin R. Bryce, and Andrew P. Monkman*

Abstract: *Two phosphorescent dinuclear iridium(III) diastereomers (ΛΔ/ΔΛ) and (ΛΛ/ΔΔ) are readily separated by making use of their different solubilities in hot hexane. The bridging diarylhydrazide ligand plays an important role in the electrochemistry and photophysics of the complexes. Organic light-emitting devices (OLEDs) that use these complexes as the green-emissive dopants in solution-processable single-active-layer architectures feature electroluminescence efficiencies that are remarkably high for dinuclear metal complexes, achieving maximum values of 37 cd A^{-1}, 14 lm W^{-1}, and 11 % external quantum efficiency.*

Emitters with high luminous efficiency are essential for full-color organic light-emitting diode (OLED) displays[1] and white light sources.[2] Phosphorescent heavy-metal complexes provide high electroluminescence (EL) efficiencies by harvesting both singlet and triplet electrogenerated excitons in the emitting layer.[1b,3–5] Cyclometalated iridium(III) complexes are widely exploited because of their excited-state lifetimes on the microsecond time scale, high quantum yields, good thermal and chemical stability, and tunability of the emission color.[6–10] In this context, the prototype complex is *fac*-[Ir(ppy)$_3$] (ppy = 2-phenylpyridine).

The photoluminescence quantum yields of dinuclear metal complexes[11–25] are usually considerably lower than those of their mononuclear analogues[12,14,23,24] (although there are exceptions),[25] leading to the established view that dinuclear complexes give poor device performance.[26,27] For example, the quantum yield of the bis(μ-Cl) bridged dimer [{Ir(ppy)$_2$Cl}$_2$] (**1**) is only 0.5 %,[11] whereas that of *fac*-[Ir(ppy)$_3$] is 40(±0.1) % (both in toluene).[28] Consequently, the vast majority of phosphorescent OLED (PhOLED) studies have used mononuclear complexes.[1b] However, dinuclear complexes are attractive as their luminescence properties can be tuned by variation of the bridge and the cyclometalated ligands.[29]

Varying the bridging ligands to provide new diiridium systems is a largely unexplored topic. We now report the new diastereomeric complexes **3** and **4** and establish that the two diastereomers **3** (ΛΔ/ΔΛ) and **4** (ΛΛ/ΔΔ) can be readily separated. Using complex **4** as the dopant in a simple solution-processed PhOLED architecture gave efficiencies of 37 cd A^{-1}, 14 lm W^{-1}, and 11 % external quantum efficiency (EQE). To the best of our knowledge, these are the highest reported efficiencies for PhOLEDs using a bimetallic complex as the emitter.

Reaction of **1**[28] with **2** gave the two diastereomers **3** (ΛΔ/ΔΛ, 41 % yield) and **4** (ΛΛ/ΔΔ, 30 % yield; Scheme 1; see also the Supporting Information, Chart S1) which were readily separated by making use of their different solubilities in hot hexane. The dimethoxy analogue **5** (ΔΛ, 43 % yield) was similarly obtained and is included here as its crystal structure was obtained with higher precision than that of **3**. The structures of **3**–**5** were established by ^{1}H NMR spectroscopy, mass spectrometry, elemental analysis, and single-crystal X-ray diffraction. There are two unique ppy groups in **3**, **4**, and **5**, as confirmed by the aromatic regions of their ^{1}H NMR spectra (Figure 1; see also S1, S3, and S5). The peaks for the two different pyridine rings (A and B) and the two phenylene rings (C and D) were assigned with the aid of ^{1}H–^{1}H 2D COSY spectra (Figure S2 and S4). Whereas studies[21,22,30] on the enantiomer separation of monoiridium complexes have been reported, the facile separation of diastereomers of a diiridium complex into their pure forms, such as complexes **3** and **4**, has, to the best of our knowledge, not been demonstrated previously.

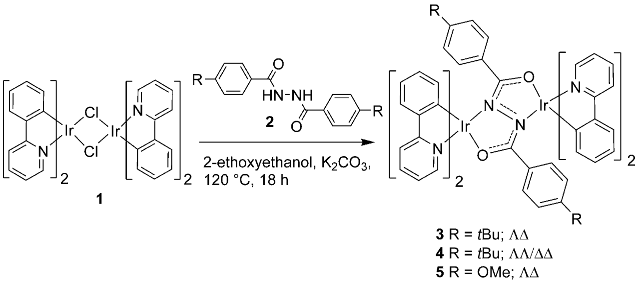

Scheme 1. Synthesis of the complexes **3**–**5**.

---

[*] Dr. Y. Zheng, Dr. A. S. Batsanov, Dr. M. A. Fox, Prof. M. R. Bryce
Department of Chemistry, Durham University
Durham DH1 3LE (UK)
E-mail: m.r.bryce@durham.ac.uk
Dr. H. A. Al-Attar, K. Abdullah, Dr. V. Jankus, Prof. A. P. Monkman
Department of Physics, Durham University
Durham DH1 3LE (UK)

[**] We thank the EPSRC for funding and Dr. E. Pohl for access to the Bruker MicroStar rotating anode.

Supporting information for this article is available on the WWW under http://dx.doi.org/10.1002/anie.201407475.

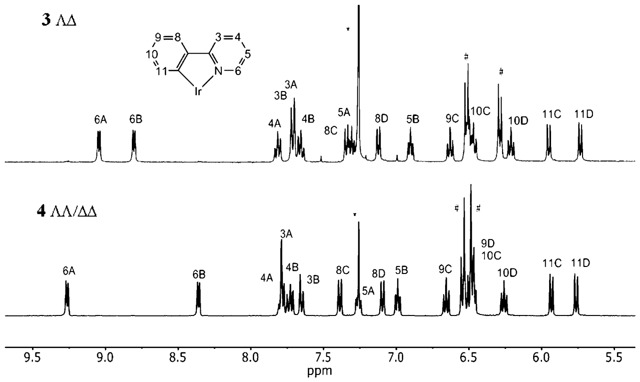

Figure 1. Aromatic regions in the ^{1}H NMR spectra for **3** and **4**. Peaks marked * are from residual CHCl$_3$ in CDCl$_3$, and peaks marked # are assigned to the aromatic protons of the tBuC$_6$H$_4$ group.

The electrochemical properties of **3** and **4** were examined by cyclic voltammetry in dichloromethane (CH$_2$Cl$_2$) solutions. The complexes show two reversible oxidation waves, which were assigned to the formally Ir^{III}/Ir^{IV}-based processes at $E_{1/2}{}^{ox} = 0.22$ V and 0.62 V (vs. FcH/FcH$^+$, FcH = ferrocene; Figure S6 and Table S1) with peak splitting on the oxidative and reductive scans in the range of 75–90 mV. The appearance of two waves that are separated by approximately 400 mV is consistent with the involvement of the bridge in the first oxidation process as the two Ir···Ir centers are 5.1 Å apart.

The crystal structure of **3** gives the ΛΔ configuration for independent molecules **A** and **B** (Figure 2). As the precision was limited by the quality of the crystals, the structure (ΛΔ) of analogue **5** (Figure S7) was also determined. The crystal of **4** contains inversion-related ΔΔ (Figure 2) and ΛΛ isomers; the molecule has approximate local C_2 symmetry but no crystallographic symmetry. The two linear N(py)–Ir–N(py) fragments are staggered by 59.3° in molecule **4**, but nearly parallel in **3** (to within 7.3° and 0.5°) and **5** (1.0°).[31]

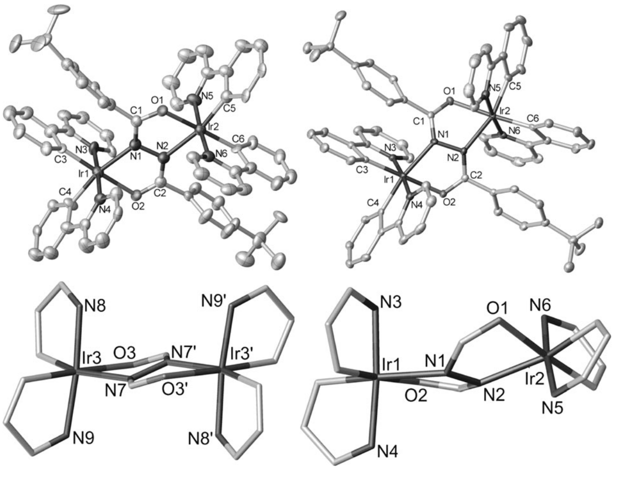

Figure 2. X-ray molecular structures of **3** (left; molecule **A**) and **4** (right). Primed atoms are generated by an inversion center. Thermal ellipsoids are set at the 50% probability level; hydrogen atoms are omitted for clarity. Core parts of **3** (left; molecule **B**) and **4** (right) in the X-ray structures.

The computed frontier molecular orbitals for the optimized geometries of **3** and **4** reveal the HOMOs to be of bridge (49–50%) and metal character (36%), as expected from the large separation of the two oxidation waves in their CV data (Figure 3, S12, and S13; Table S5–S7). The LUMOs are located at the ppy ligands. The bridge involvement in the HOMOs of **3** and **4** contrasts with the HOMO of **1**, which is located on the metal and the phenylene unit of the ppy ligand. We are not aware of a previous computational study on diiridium complexes where the bridge has been shown to be heavily involved in the HOMO: Typically, either the LUMO involves bridge character,[16,18,23,32] or the bridge is not involved in either frontier orbital.[19,24]

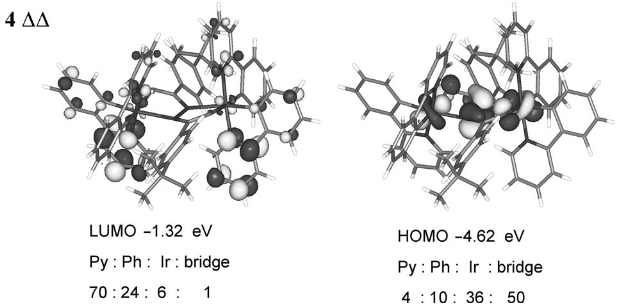

Figure 3. Frontier orbitals for the optimized geometry of **4**.

The photophysical data for **2**, **3**, and **4** are shown in Figures S8 and S9 and Tables S3 and S4; data for [Ir(ppy)$_3$] and **1** obtained under directly comparable conditions are included for comparison. The PL emissions of **3** and **4** at 521 nm and 523 nm are featureless, which indicates a dominant ^{3}MLCT contribution and little signature of ^{3}LC contribution. The luminescence quantum yields of **3** and **4** in CH$_2$Cl$_2$ solutions were 71% and 88%, whereas when the complexes were blended in zeonex at a concentration of 5% w/w, the quantum yields were determined to be 38% and 41%, respectively. These are unusually high quantum yields for diiridium complexes and are comparable to those of [Ir(ppy)$_3$] [40% in both CH$_2$Cl$_2$ (this work) and in toluene].[28] The phosphorescence decays of **3** and **4** doped in zeonex at 5% (Figure S10) show very similar lifetimes to that of [Ir(ppy)$_3$] (ca. 1.4 μs), which is consistent with emission from a triplet excited state. The emission of **3** and **4** in CH$_2$Cl$_2$ solution (λ_{max} 521–523 nm) is red-shifted compared to the emission of [Ir(ppy)$_3$] (510 nm).

Devices were fabricated by spin coating to give the single-active-layer structure ITO/PEDOT:PSS (50 nm)/[PVK:PBD (40%):Ir complex (5%)] (90 nm)/Ba (4 nm)/Al (100 nm). Figure 4 and Figures S14–S16 show the device characteristics for complexes **1**, **3**, and **4**. Figures 4 and S16 and Table 1 also include data for the previously reported bis(μ-Cl) bridged diiridium complex with cyclometalated fluorenylpyridine (flpy) as the C,N ligands, [{Ir(flpy)$_2$Cl}$_2$] (Chart S2).[24] This complex is used for comparison as it has a similar solubility to complex **4**. Complex **4** displays very high performance, with an EQE of 11% and a current efficiency of 37 cd A^{-1}, compared to 7% and 24 cd A^{-1} for **3**. To the best of our

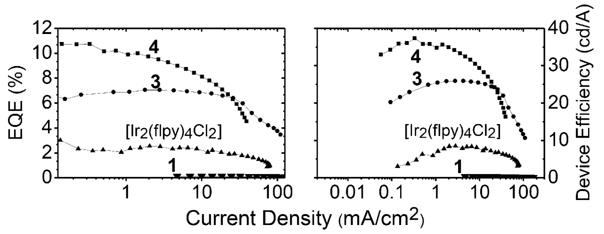

Figure 4. Device characteristics of complexes **1**, **3**, **4**, and [{Ir(flpy)$_2$Cl}$_2$] for a dopant concentration of 5% w/w. Data for [{Ir(flpy)$_2$Cl}$_2$] were taken from Ref. [24].

Table 1: Turn-on voltage and maximum device efficiencies for **1**, **3**, **4**, and [{Ir(flpy)$_2$Cl}$_2$].

Complex	Turn-on voltage [V] at 1 cd m^{-2}	EQE [%]	Current efficiency [cd A^{-1}]	Maximum brightness [cd m^{-2}]	Power efficiency [lm W^{-1}]	Maximum radiant power [mW]
1	8	0.15	0.35	220	0.12	0.05
3	6.2	7	24	11 000	7	0.8
4	5.5	11	37	7000	14	1.8
fac-[{Ir(flpy)$_2$Cl}$_2$][24]	4.7	2.5	8.5	3000	3	0.4

knowledge, these values for **4** are the highest values that have been reported for solution-processed devices of diiridium complexes to date, and they are significantly higher than the previously highest values of 4% and 12 cd A^{-1} reported for [Ir$_2$(flpy)$_4$Cl$_2$] (2.5% and 8.5 cd A^{-1} under the same conditions as used for devices **3** and **4**).[24] The enhanced device efficiency of complex **4** compared to that of **3** may be explained by the increased solubility of **4** and the different film morphologies, which are based on the different molecular conformations of **3** and **4** (Figure 2). It is noteworthy that complex **4** has an even higher device efficiency than the benchmark green emitter [Ir(ppy)$_3$] at a dopant concentration of 5% for a device obtained by single-active-layer solution processing.[33]

To probe the reasons for the high efficiency of these diiridium PhOLEDs, the EL transient of the device ITO/PEDOT:PSS/[PVK: PBD (40%): complex **3** (5%)]/Ba/Al was compared with the photoluminescence (PL) transient (Figure S18a). The first feature, which lasts from 0.1 μs to 10 μs, is a single exponential with a lifetime of approximately 1.4 μs, and the second feature, which lasts from 10 μs to 1 ms, is a power law with a slope of approximately −0.6. Time-resolved spectra (Figure S18b) recorded between 900–1500 ns (during exponential decay) and between 140–160 μs (during the power-law decay) are identical, indicating that both features are due to the same emissive state of **3**. The lifetime of the emissive state is only 1.45 μs (Table S4); thus at later times, it must be fed from another state thereby substantially increasing the EL. To the best of our knowledge, similar power-law features have not been reported previously for iridium-based PLEDs.

In conclusion, three special features of this work are: 1) the two diastereomeric complexes **3** (ΛΔ/ΔΛ) and **4** (ΛΛ/ΔΔ) are readily separated; 2) the bridging ligands are non-innocent; and 3) complex **4** gives green PhOLEDs with efficiencies of 37 cd A^{-1}, 14 lm W^{-1}, and 11% EQE, which are remarkably high values for dinuclear metal complexes. There is considerable scope for exploring new diiridium complexes, especially with conjugated or non-innocent bridging ligands, to probe interactions between the metal centers, to achieve color tuning, and to obtain highly efficient OLEDs.

Received: July 22, 2014

Keywords: diastereomers · iridium · ligand design · luminescence · OLEDs

[1] a) *Organic Light-Emitting Devices* (Eds.: K. Müllen, U. Scherf), Wiley-VCH, Weinheim, **2006**; b) *Highly Efficient OLEDs with Phosphorescent Materials* (Ed.: H. Yersin), Wiley-VCH, Weinheim, **2008**, chap. 8; c) S. Y. Lee, T. Yasuda, Y. S. Yang, Q. Zhang, C. Adachi, *Angew. Chem. Int. Ed.* **2014**, *53*, 6402–6406; *Angew. Chem.* **2014**, *126*, 6520–6524.
[2] For a review, see: a) K. T. Kamtekar, A. P. Monkman, M. R. Bryce, *Adv. Mater.* **2010**, *22*, 572–582; for an example, see: b) W.-X. Ni, M. Li, J. Zheng, S.-Z. Zhan, Y.-M. Qiu, S. W. Ng, D. Li, *Angew. Chem. Int. Ed.* **2013**, *52*, 13472–13476; *Angew. Chem.* **2013**, *125*, 13714–13718.
[3] M. A. Baldo, D. F. O'Brien, Y. You, A. Shoustikov, S. Sibley, M. E. Thompson, S. R. Forrest, *Nature* **1998**, *395*, 151–154.
[4] Y. Kawamura, K. Goushi, J. Brooks, J. J. Brown, H. Sasabe, C. Adachi, *Appl. Phys. Lett.* **2005**, *86*, 071104.
[5] X.-C. Hang, T. Fleetham, E. Turner, J. Brooks, J. Li, *Angew. Chem. Int. Ed.* **2013**, *52*, 6753–6756; *Angew. Chem.* **2013**, *125*, 6885–6888.
[6] S. Lamansky, P. Djurovich, D. Murphy, F. Abdel-Razzaq, H.-E. Lee, C. Adachi, P. E. Burrows, S. R. Forrest, M. E. Thompson, *J. Am. Chem. Soc.* **2001**, *123*, 4304–4312.
[7] For a review, see: E. Holder, B. M. W. Langeveld, U. S. Schubert, *Adv. Mater.* **2005**, *17*, 1109–1121.
[8] For a review, see: L. Xiao, Z. Chen, B. Qu, J. Luo, S. Kong, Q. Gong, J. Kido, *Adv. Mater.* **2011**, *23*, 926–952.
[9] N. Tian, D. Lenkeit, S. Pelz, D. Kourkoulos, D. Hertel, K. Meerholz, E. Holder, *Dalton Trans.* **2011**, *40*, 11629–11635.
[10] D. Xia, B. Wang, B. Chen, S. Wang, B. Zhang, J. Ding, L. Wang, X. Jing, F. Wang, *Angew. Chem. Int. Ed.* **2014**, *53*, 1048–1052; *Angew. Chem.* **2014**, *126*, 1066–1070.
[11] G. A. Carlson, P. I. Djurovich, R. J. Watts, *Inorg. Chem.* **1993**, *32*, 4483–4484.
[12] A. Tsuboyama, T. Takiguchi, S. Okada, M. Osawa, M. Hoshino, K. Ueno, *Dalton Trans.* **2004**, 1115–1116.
[13] E. A. Plummer, J. W. Hofstraat, L. De Cola, *Dalton Trans.* **2003**, 2080–2084.
[14] A. Santoro, A. M. Prokhorov, V. N. Kozhevnikov, A. C. Whitwood, B. Donnio, J. A. G. Williams, D. W. Bruce, *J. Am. Chem. Soc.* **2011**, *133*, 5248–5251.
[15] V. Chandrasekhar, S. M. W. Rahaman, T. Hajra, D. Das, T. Ghatak, S. Rafiq, P. Sen, J. K. Bera, *Chem. Commun.* **2011**, *47*, 10836–10838.
[16] E. S. Andreiadis, D. Imbert, J. Pécaut, A. Calborean, I. Ciofini, C. Adamo, R. Demadrille, M. Mazzanti, *Inorg. Chem.* **2011**, *50*, 8197–8206.
[17] E. Baranoff, E. Orselli, L. Allouche, D. Di Censo, R. Scopelliti, M. Grätzel, M. D. Nazeeruddin, *Chem. Commun.* **2011**, *47*, 2799–2801.

[18] V. Chandrasekhar, T. Hajra, J. K. Bera, S. M. W. Rahaman, N. Satumitra, O. Elbjeirami, M. A. Omary, *Inorg. Chem.* **2012**, *51*, 1319 – 1329.
[19] V. Chandrasekhar, B. Mahanti, P. Bandipalli, K. Bhanuprakash, *Inorg. Chem.* **2012**, *51*, 10536 – 10547.
[20] V. L. Whittle, J. A. G. Williams, *Inorg. Chem.* **2008**, *47*, 6596 – 6607.
[21] A. Auffrant, A. Barbieri, F. Barigelletti, J. Lacour, P. Mobian, J.-P. Collin, J.-P. Sauvage, B. Ventura, *Inorg. Chem.* **2007**, *46*, 6911 – 6919.
[22] M. Graf, R. Czerwieniec, K. Sünkel, *Z. Anorg. Allg. Chem.* **2013**, *639*, 1090 – 1094.
[23] L. Donato, C. E. McCusker, F. N. Castellano, E. Zysman-Colman, *Inorg. Chem.* **2013**, *52*, 8495 – 8504.
[24] A. M'hamedi, A. S. Batsanov, M. A. Fox, M. R. Bryce, K. Abdullah, H. A. Al-Attar, A. P. Monkman, *J. Mater. Chem.* **2012**, *22*, 13529 – 13540.
[25] P.-H. Lanoë, C. M. Tong, R. W. Harrington, M. R. Probert, W. Clegg, J. A. G. Williams, V. N. Kozhevnikov, *Chem. Commun.* **2014**, *50*, 6831 – 6834.
[26] S. Bettington, M. Tavasli, M. R. Bryce, A. S. Batsanov, A. L. Thompson, H. A. Al Attar, F. B. Dias, A. P. Monkman, *J. Mater. Chem.* **2006**, *16*, 1046 – 1052.
[27] X. Li, D. Zhang, W. Li, B. Chu, L. Han, T. Li, Z. Su, J. Zhu, Y. Chen, Z. Hu, P. Lei, Z. Zhang, *Opt. Mater.* **2009**, *31*, 1173 – 1176.
[28] K. A. King, P. J. Spellane, R. J. Watts, *J. Am. Chem. Soc.* **1985**, *107*, 1431 – 1432.
[29] V. W.-W. Yam, K. M.-C. Wong, *Chem. Commun.* **2011**, *47*, 11579 – 11592.
[30] a) C. Schaffner-Hamann, A. von Zelewsky, A. Barbieri, F. Barigelletti, G. Muller, J. P. Riehl, A. Neels, *J. Am. Chem. Soc.* **2004**, *126*, 9339 – 9348; b) C. Hamann, A. von Zelewsky, A. Neels, H. Stoeckli-Evans, *Dalton Trans.* **2004**, 402 – 406; c) F. J. Coughlin, M. S. Westrol, K. D. Oyler, N. Byrne, C. Kraml, E. Zysman-Colman, M. S. Lowry, S. Bernhard, *Inorg. Chem.* **2008**, *47*, 2039 – 2048; d) E. Marchi, R. Sinisi, G. Bergamini, M. Tragni, M. Monari, M. Bandini, P. Ceroni, *Chem. Eur. J.* **2012**, *18*, 8765 – 8773.
[31] CCDC 995196 (complex **3**), 995198 (complex **4**), and 995197 (complex **5**) contain the supplementary crystallographic data for this paper. These data can be obtained free of charge from The Cambridge Crystallographic Data Centre via www.ccdc.cam.ac.uk/data_request/cif.
[32] A. M. Soliman, D. Fortin, P. D. Harvey, E. Zysman-Colman, *Dalton Trans.* **2012**, *41*, 9382 – 9393.
[33] H. A. Al-Attar, G. C. Griffiths, T. N. Moore, M. Tavasli, M. A. Fox, M. R. Bryce, A. P. Monkman, *Adv. Funct. Mater.* **2011**, *21*, 2376 – 2382.